J|A|C|S
ARTICLES

Published on Web 10/17/2008

Role of the Hydrophobic Effect in the Transfer of Chirality from Molecules to Complex Systems: From Chiral Surfactants to Porphyrin/Surfactant Aggregates

Zoubir El-Hachemi,[§] Giovanna Mancini,*[,†,‡] Josep M. Ribó,*[,§] and Alessandro Sorrenti[†]

Dipartimento di Chimica, and CNR, Istituto di Metodologie Chimiche, Sezione Meccanismi di Reazione and Dipartimento di Chimica, Università degli Studi di Roma "La Sapienza", P.le A Moro 5, 00185 Roma, Italy, and Departament de Química Orgànica, Universitat de Barcelona, c/Martì Franquès 1, 08028 Barcelona, Spain

Received July 21, 2008; E-mail: giovanna.mancini@uniroma1.it; jmribo@ub.edu

Abstract: The interaction between the achiral sulfonated porphyrin 5,10,15,20-tetrakis(4-sulfonatophenyl)porphyrin, $H_2TPPS_4^{4-}$, and two chiral cationic surfactants has been studied by optical absorption, fluorescence, and circular dichroism (CD) spectroscopies. At surfactant concentrations above the critical micellar concentration (cmc) the porphyrin is included in the micellar aggregates, but it is CD silent. Below the cmc at a definite porphyrin/surfactant stoichiometry the formation of heteroaggregates with transfer of chirality to the porphyrin chromophore occurs. The preferred surfactant/porphyrin stoichiometry is 3:1, which suggests a structure driven by electrostatic and hydrophobic interactions between porphyrin and surfactant and dipolar and ionic interactions with the water solution. At surfactant concentrations above the cmc, depending on the protocol of preparation of the samples, the formation of the two kinds of aggregates can be observed, reversible for the simple surfactant micelles incorporating the porphyrin, but irreversible for the heteroaggregates.

Introduction

Chirality is observed in nature at different levels of complexity, from molecules to the macroscopic level of biological systems, such as snails, flowers, and twining vines.[1] Most chiral species are present in nature only in one of the enantiomeric forms; at molecular level, for example, racemic mixtures of biomolecules and biopolymers are excluded to form part of the basic processes that define life. Fundamental discussions on this suggest that the biological homochirality could be a consequence of the atom "homochirality" arising from the violation of the parity of the electroweak force.[2] Independently from this basic issue, there are the pure chemical topics of the transfer of chirality and of the chiral amplification in the building of biological complex systems from simple molecules. The study of transfer of chirality in the self-assembly of hierarchical supramolecular associates can give basic knowledge on this.[3]

The transfer and amplification of chirality has been studied on chiral porphyrins.[4] Achiral porphyrins have been used to detect chirality by the formation of heteroassociates with chiral compounds[5,6] or by the formation, in spontaneous symmetry-breaking processes, of chiral homoassociates whose chiral sign is determined by the influence of weak chiral polarizations.[3d,i] In fact, porphyrins are some of the most powerful and versatile

[†] Dipartimento di Chimica, Università degli Studi di Roma "La Sapienza".

[‡] Istituto di Metodologie Chimiche, Sezione Meccanismi di Reazione, Università degli Studi di Roma "La Sapienza".

[§] Universitat de Barcelona.

(1) Janoschek, R., Ed. *Chirality—From Weak Bosons to the α-Helix*; Springer Verlag: Berlin, 1991.

(2) (a) Zanasi, R.; Lazzaretti, P.; Ligabue, A.; Soncini, A. *Phys. Rev. E* **1999**, *59*, 3382–3385. (b) Lazzaretti, P.; Zanasi, R.; Faglioni, F. *Phys. Rev. E* **1999**, *60*, 871–874. (c) Berger, R.; Quack, M. *ChemPhysChem* **2000**, *1*, 57–60. (d) Johnson, L. N. *Eur. Rev.* **2005**, *13*, 77–95. (e) Fitz, D.; Reiner, H.; Plankensteiner, K.; Rode, B. M. *Curr. Chem. Biol.* **2007**, *1*, 41–52.

(3) (a) Laursen, R. A.; Wen, D.; Knight, C. A. *J. Am. Chem. Soc.* **1994**, *116*, 12057–12058. (b) Orme, C. A.; Noy, A.; Wierzbicki, A.; McBride, M. T.; Grantham, M.; Teng, H. H.; Dove, P. M.; De Yoreo, J. J. *Nature* **2001**, *411*, 775–779. (c) De Feyter, S.; Gesquière, A.; Wurst, K.; Amabilino, D. B.; Veciana, J.; De Schryver, F. C. *Angew. Chem.* **2001**, *113*, 3317–3320. (d) Ribó, J. M.; Crusats, J.; Sagués, F.; Claret, J.; Rubires, R. *Science* **2001**, *292*, 2063–2066. (e) Zepik, H.; Shavit, E.; Tang, M.; Jensen, T. R.; Kjaer, K.; Bolbach, G.; Leiserowitz, L.; Weissbuch, I.; Lahav, M. *Science* **2002**, *295*, 1266–1269. (f) Geva, M.; Frolow, F.; Eisenstein, M.; Addadi, L. *J. Am. Chem. Soc.* **2003**, *125*, 696–704. (g) Levy-Lior, A.; Weiner, S.; Addadi, L. *Helv. Chim. Acta* **2003**, *86*, 4007–4017. (h) Purrello, R. *Nat. Mater.* **2003**, *2*, 216–217. (i) Crusats, J.; Claret, J.; Diez-Perez, I.; El-Hachemi, Z.; Garcı´a-Ortega, H.; Rubires, R.; Sagués, F.; Ribó, J. M. *J. Chem. Soc., Chem. Commun.* **2003**, *158*, 8–1589. (j) Zhang, L.; Yuan, J.; Liu, M. *J. Phys. Chem. B* **2003**, *107*, 12768–12773. (k) Mateos-Timoneda, M. A.; Crego-Calama, M.; Reinhoudt, D. N. *Chem. Soc. Rev* **2004**, *33*, 363–372. (l) Zhang, Y.; Chen, P.; Liu, M. *Chem. Eur. J.* **2008**, *14*, 1793–1803.

(4) (a) Monti, D.; Venanzi, M.; Mancini, G.; Di Natale, C.; Paolesse, R. *Chem. Commun.* **2005**, 2471–2743. (b) Monti, D.; Venanzi, M.; Stefaneli, M.; Sorrenti, A.; Mancini, G.; Di Natale, C.; Paolesse, R. *J. Am. Chem. Soc.* **2007**, *129*, 6688–6689. (c) Monti, D.; Cantonetti, V.; Venanzi, M.; Bombelli, C.; Ceccacci, F.; Mancini, G. *Chem. Commun.* **2004**, 972–973. (d) Štěpánek, P.; Dukh, M.; Šaman, D.; Moravcová, J.; Kniežo, L.; Monti, D.; Venanzi, M.; Mancini, G.; Drašar, P. *Org. Biomol. Chem.* **2007**, *5*, 960–970. (e) Fuhrhop, J. H.; Demoulin, C.; Boettcher, C.; Koning, J.; Siggel, U. *J. Am. Chem. Soc.* **1992**, *114*, 4159–4165.

 10.1021/ja805669v CCC: $40.75

Chart 1

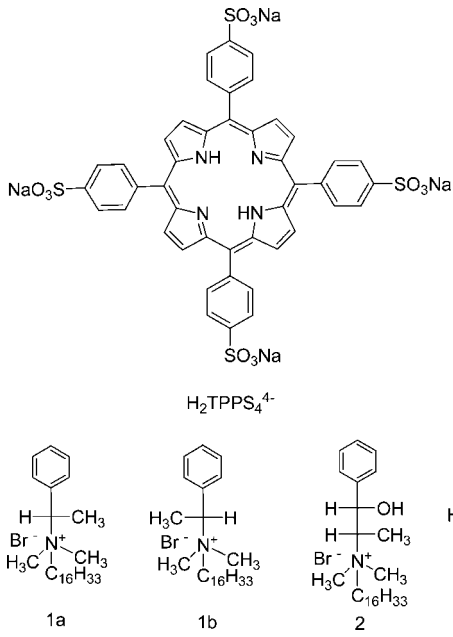

probes to gain information on the structure and on the chirality of the systems where they are embedded.[4−7]

Here we report on the formation of different kinds of aggregates formed by the tetrasodium salt of the achiral water-soluble 5,10,15,20-tetrakis(4-sulfonatophenyl)porphyrin, $H_2TPPS_4^{4-}$, with chiral cationic surfactants: the enantiomers of *N*,*N*-dimethyl-*N*-(1-phenylethyl)hexadecan-1-ammonium bromide, **1a** and **1b**, and (1*S*,2*S*)-*N*-(2-hydroxy-1-methyl-2-phenylethyl)-*N*,*N*-dimethylhexadecan-1-ammonium bromide, **2** (Chart 1). The methodology used was based on the porphyrin chromophore as target of absorption (UV−vis and circular dichroism) and emission spectroscopy.

It is known that the interaction of porphyrins with surfactants can give different systems depending upon the [surfactant]/[porphyrin] ratio and the nature of the two species.[8] At high [surfactant]/[porphyrin] ratios the inclusion of monomeric porphyrin in surfactant micellar aggregates is generally observed, whereas at low ratios the formation of so-called premicellar surfactant−porphyrin aggregates is observed.[8c−f] However, to the best of our knowledge, studies on the interaction between achiral anionic porphyrins and chiral cationic surfactants have not been reported. The investigation of these systems might give insights into the mechanisms of transfer of the chiral information from the molecular level to the nanoscale level of polymolecular aggregates.

Materials and Methods

The tetrasodium salt of 5,10,15,20-tetrakis(4-sulfonatophenyl)porphyrin $H_2TPPS_4^{4-}$ ($Na_4H_2TPPS_4$) was prepared as previously reported.[9]

(*S*)- and (*R*)-*N*,*N*-Dimethyl-*N*-(1-phenylethyl)hexadecan-1-ammonium bromide (**1a** and **1b**) were prepared according to a reported procedure.[10] ^{1}H NMR, δ ($CDCl_3$): 0.833 (t, CH_3, 3H, $J = 6.5$ Hz), 1.249 (m, CH_2 chain, 26H), 1.783 (m, CH_2, 2H), 1.830 (d, CH_3, 3H, $J = 7.1$ Hz), 3.160 (s, CH_3, 3H), 3.200 (s, CH_3, 3 H), 3.470 (t, CH_2, 2H, $J = 7.1$ Hz), 5.389 (q, CH, 1H $J = 7.1$ Hz), 7.38−7.47 (m, ar, 3H), 7.620 (m, ar, 2H).

(1*S*,2*S*)-*N*-(2-Hydroxy-1-methyl-2-phenylethyl)-*N*,*N*-dimethylhexadecan-1-ammonium bromide, **2**, was prepared according to a reported procedure.[10] ^{1}H NMR, δ ($CDOD_3$): 0.894 (t, CH_3, 3H, $J = 6.7$ Hz), 1.090 (d, CH_3, 3H, $J = 6.7$ Hz), 1.289 (m, CH_2 chain, 26H), 1.800 (m, CH_2, 1H), 1.943 (m, CH_2, 1H), 3.220 (s, CH_3, 3H), 3.292 (s, CH_3, 3H), 3.525 (m, N^+CH_2, 1H), 3.732 (m, N^+CH_2, 1H), 3.911 (m, CH, 1H), 4.910 (d, CH, 1H, $J = 9.9$ Hz), 7.33−7.48 (m, ar, 5H).

(*R*)-*N*,*N*,*N*-Trimethyl-1-phenylethanammonium bromide, **3**, was prepared as follows. An amount of 228 mg of CH_3I (1.6 mmol) was added to a solution of 130 mg (0.88 mmol) of (*R*)-*N*,*N*-dimethyl-1-phenylethylamine in 1 mL of methanol; the reaction mixture was kept under stirring at room temperature for 2 days. The iodide salt was precipitated from methanol by Et_2O, filtered, and washed with Et_2O. The bromide salt was obtained by dissolving the iodide salt in a methanol solution saturated with NaBr. Purification by chromatography on silica gel ($CHCl_3$/MeOH = 80/20) of the residue obtained after filtration of the solution and removal of the solvent under vacuum yielded the pure product, as a light yellow solid. ^{1}H NMR, δ (CD_3OD): 1.823 (d, CH_3, 3H, $J = 7.0$ Hz), 3.140 (s, CH_3, 9H), 4.890 (q, CH, 1H $J = 7.0$ Hz), 7.50−7.53 (m, ar, 3H), 7.63−7.66 (m, ar, 2H).

Water of Millipore Q quality (18.2 MΩ cm) was used for the preparation of all the aqueous solutions.

Instrumentation. Conductivity measurements were carried out at 298 K on a Hanna conductimeter HI-9932, equipped with a thermostatting apparatus.

Circular dichroism (CD) spectra were recorded on Jasco spectropolarimeters J-715 and J-810.

UV−vis spectra were recorded on a Carey-300 UV−vis spectrophotometer. The spectral changes induced by the increase of temperature were recorded by Varian-Carey (500 SCAN) UV−vis−NIR spectrophotometer equipped with a Peltier temperature controller.

Fluorescence spectra were recorded on a PTI spectrofluorimeter in L geometry equipped with a Xe lamp (LPS 220B) and a photomultiplier detection system PTI 814.

Resonance light scattering measurements[5c,13] were carried out on a Horiba Jobin Yvon Fluoromax-4 spectrofluorimeter, with a right angle geometry, by operating in the synchronous scanning mode in which the excitation and emission monochromators are coupled to scan simultaneously.

Determination of Critical Micellar Concentration. Critical micellar concentration (cmc) of surfactant **2** was measured by conductivity experiments according to a described procedure.[11] Known volumes of 25 mM aqueous solution of surfactant were

(5) (a) Bellacchio, E.; Lauceri, R.; Guerrieri, S.; Scolaro, L. M.; Romeo, A.; Purrello, R. *J. Am. Chem. Soc.* **1998**, *120*, 12353–12354. (b) Purrello, R.; Raudino, A.; Scolaro, L. M.; Loisi, A.; Bellacchio, E.; Lauceri, R. *J. Phys. Chem. B* **2000**, *104*, 10900–10908. (c) Pasternack, R. F.; Bustamante, C.; Collings, P. J.; Giannetto, A.; Gibbs, E. J. *J. Am. Chem. Soc.* **1993**, *115*, 5393–5399. (d) Lauceri, R.; Purrello, R.; Shetty, S. J.; Graca, M.; Vicente, H. *J. Am. Chem. Soc.* **2001**, *123*, 5835–5836.

(6) Hembury, G. A.; Borovkov, V.; Inoue, Y. *Chem. Rev.* **2008**, *108*, 1–73.

(7) Pescitelli, G.; Gabriel, S.; Wang, Y.; Fleischhauer, J.; Woody, R. W.; Berova, N. *J. Am. Chem. Soc.* **2003**, *125*, 7613–7628.

(8) (a) Andrade, S. M.; Teixeira, R.; Costa, S. M. B.; Sobral, A. J. F. N. *Biophys. Chem.* **2008**, *133*, 1–10. (b) Andrade, S. M.; Costa, S. M. B. *Chem. Eur. J.* **2006**, *12*, 1046–1057. (c) Maiti, N. C.; Mazumdar, S.; Periasamy, N. *J. Phys. Chem. B* **1998**, *102*, 1528–1538. (d) Maiti, N. C.; Mazumdar, S.; Periasamy, N. *J. Porphyrins Phthalocyanines* **1998**, *2*, 369–376. (e) Gandini, S. C. M.; Yushmanov, V. E.; Borissevitch, I. E.; Tabak, M. *Langmuir* **1999**, *15*, 6233–6243. (f) Barber, D. C.; Freitag-Beeston, R. A.; Whitten, D. G. *J. Phys. Chem.* **1991**, *95*, 4074–4086.

(9) Rubires, R.; Crusats, J.; El-Hachemi, Z.; Jaramillo, T.; Valls, E.; Farrera, J.-A.; Ribo, J. M. *New J. Chem.* **1999**, 189–198.

(10) Moss, R. A.; Sunshine, W. L. *J. Org. Chem.* **1974**, *39*, 1083–1089.

(11) Frinii, M.; Michelis, B.; Zana, R. *J. Phys. Chem.* **1992**, *96*, 6095.

(12) Andreani, R.; Bombelli, C.; Borocci, S.; Lah, J.; Mancini, G.; Mencarelli, P.; Vesnaver, G.; Villani, C. *Tetrahedron: Asymmetry* **2004**, *15*, 987–994.

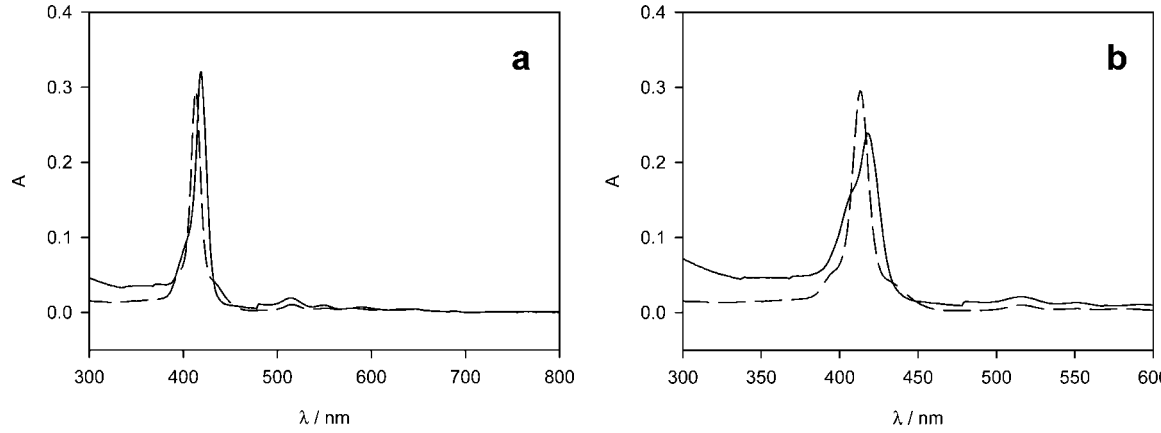

Figure 1. Soret region of the absorption spectrum of 1 μM $H_2TPPS_4^{4-}$ in the presence of surfactants **1a** (a) and **2** (b), at [surfactant]/[porphyrin] ratio of 10 000:1 (solid line), compared with the spectrum of porphyrin in water (dashed line).

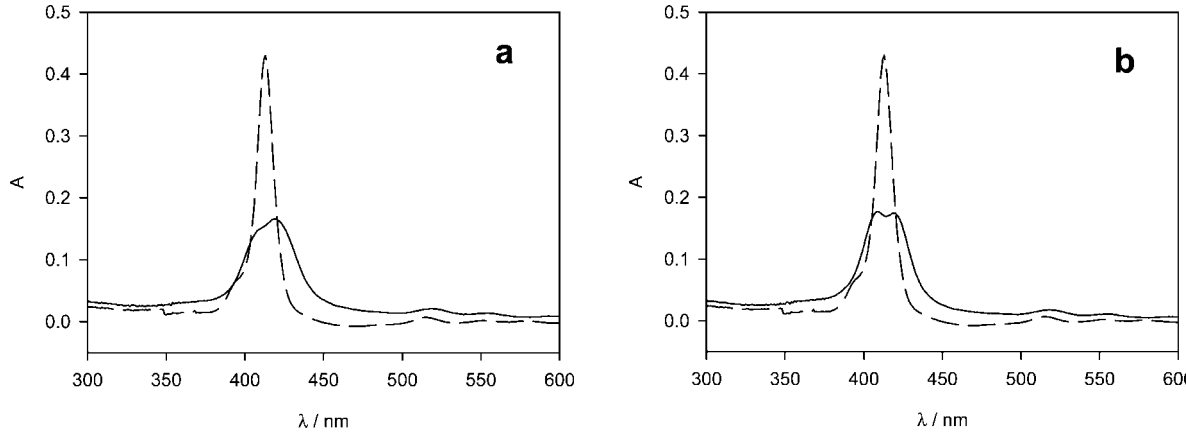

Figure 2. Soret region of the absorption spectrum of 1 μM $H_2TPPS_4^{4-}$ in the presence of surfactants **1a** (a) and **2** (b), at [surfactant]/[porphyrin] ratio of 4:1 (solid line), compared with the spectrum of porphyrin in water (dashed line).

added to a known volume of Milli-Q water. The cmc's of **1**[12] and **2** are 2.40×10^{-4} and 2.15×10^{-4} M, respectively.

Sample Preparation. Samples for UV−vis, fluorescence, and CD experiments were prepared, when not differently specified, as follow: (a) samples at [surfactant] < 1 mM were prepared by adding the necessary volume of a 0.1−1 mM porphyrin stock solution to the proper amount of water. To the resulting dilute porphyrin solution a proper amount of a stock aqueous surfactant solution was then added to obtain the required porphyrin/surfactant ratio; (b) samples at [surfactant] > 1 mM, i.e., above the cmc, were prepared by adding the proper amount of porphyrin stock solution to the surfactant solution. The concentration of the porphyrin stock solutions was checked by UV−vis spectroscopy (ε = 480.000 mol^{-1} L cm^{-1} at 413 nm).

UV−Vis and Fluorescence Experiments. Spectra were registered within 5−15 min of the sample preparation, in quartz cuvettes (path length 1 cm). Experiments were performed at room temperature, when not specified.

The stoichiometry of the porphyrin−surfactant heteroaggregate was determined by the method of continuous variations (Job's method plot analysis).[14] The total concentration of the two components (porphyrin and surfactant) was kept constant at 10 μM. The absorption spectra were recorded immediately after the preparation of the samples.

Results and Discussion

The interaction between nonchiral sulfonated porphyrin $H_2TPPS_4^{4-}$, and chiral cationic surfactants **1** and **2**, in water solution was studied by means of UV−vis spectroscopy, fluorescence, and CD spectroscopies.

The UV−vis experiments were carried out at [$H_2TPPS_4^{4-}$] = 1 μM at [surfactant]/[porphyrin] ratio ranging between 1:1 and 10 000:1 (i.e., at surfactant concentration ranging between 1 μM, well below, and 10 mM, well above, cmc), the cmc of **1** and **2** being 2.40×10^{-4} and 2.15×10^{-4} M, respectively. For the sake of clarity we report here only the UV−vis spectra relative to some selected [surfactant]/[porphyrin] ratios (Figures 1 and 2); other UV−vis spectra are reported as Supporting Information.

The absorption spectrum of $H_2TPPS_4^{4-}$ (1 μM) in pure water exhibits a sharp Soret band at 413 nm (dashed line in Figures 1 and 2) and four distinguishable Q-bands at 516, 552, 579, and 634 nm (Supporting Information). The absorption spectrum of $H_2TPPS_4^{4-}$ (at [$H_2TPPS_4^{4-}$] = 1 μM) is not affected by the presence of the chiral ammonium salt **3** (at [**3**]/[$H_2TPPS_4^{4-}$] ratios ranging between 1 and 22). Notice that this chiral ammonium salt is the homologue of surfactant **1b** with a methyl group instead of the hexadecyl hydrophobic tail. This result indicates that whatever is the interaction between these oppositely charged species, it does not perturb the porphyrin electronic transitions. On the other hand, both Soret and Q-bands of the absorbance spectrum of $H_2TPPS_4^{4-}$ are strongly affected by the presence of the cationic surfactants **1a**, **1b**, and **2** indicating a significant interaction with the charged porphyrin. For example, at [**1a**]/[$H_2TPPS_4^{4-}$] = 10 000:1 for 1 μM $H_2TPPS_4^{4-}$ the Soret band shows a red shift to 419 nm (Figure

(13) PasternacK, R. F.; Collings, P. J. *Science* **1995**, *269*, 935.
(14) Job, P. *Ann. Chim.(Paris)* **1928**, *9*, 113–203.

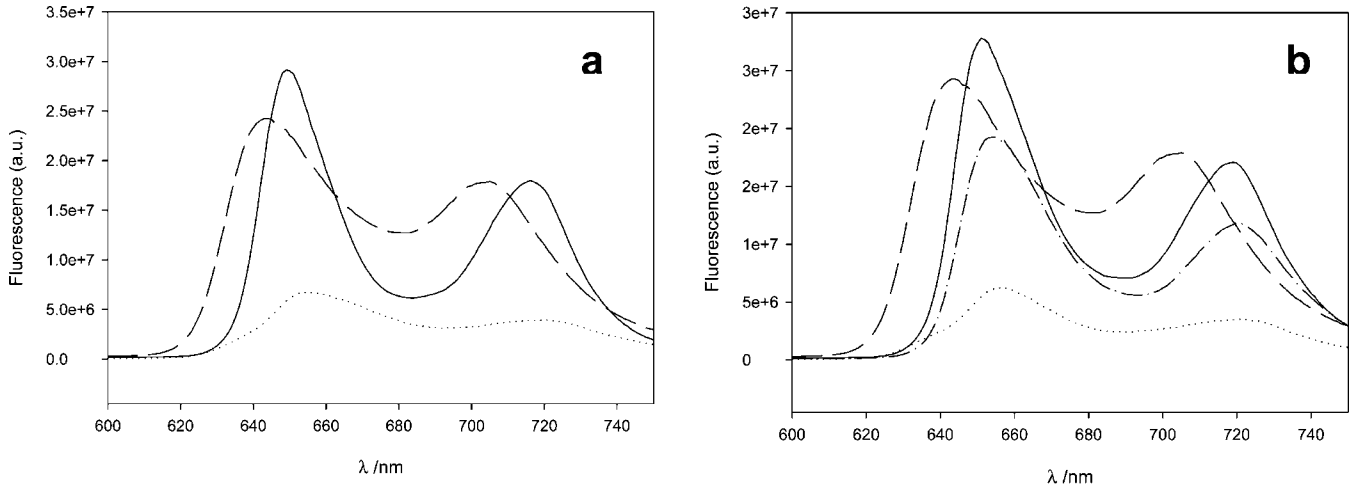

Figure 3. Fluorescence emission spectra of 1 μM $H_2TPPS_4^{4-}$ in water (panels a and b, dashed line) and in the presence of (a) surfactant **1a** at [surfactant]/[porphyrin] ratio of 4:1, λ_{ex} 408 nm (dotted line), at surfactant/porphyrin ratio of 10 000:1, λ_{ex} = 413 nm (solid line); (b) surfactant **2** at [surfactant]/[porphyrin] ratio of 4:1, λ_{ex} 408 nm (dotted line), at [surfactant]/[porphyrin] ratio of 10 000:1, λ_{ex} 407 nm (dash-dotted line), and λ_{ex} = 420 nm (solid line).

1a), which indicates the incorporation of the porphyrin in the surfactant cationic micelles. The presence of monomeric porphyrin included in micellar aggregates (micellized monomeric porphyrin) has been reported previously.[8] On the other hand, at lower [surfactant]/[porphyrin] ratios the Soret band shows a broad shape (Supporting Information), that cannot be assigned to the presence of either free porphyrin in water or micellized porphyrin, because the maximum absorptions, also those of Q(0,0) band, appear to slightly different wavelengths with respect to those of the free porphyrin and of the porphyrin incorporated in the surfactant micelles (Supporting Information). In the case of surfactant **2** the band relative to this species is also clearly observable in the absorption spectrum of $H_2TPPS_4^{4-}$ at [surfactant]/[porphyrin] ratio of 10 000:1 as a shoulder at lower wavelengths of the absorbance of micellized porphyrin (Figure 1b), whereas the single sharp band of micellized porphyrin is observed in the case of surfactant **2** only at higher [surfactant]/[porphyrin] ratio (Supporting Information). Finally, the lack of an isosbestic point in the UV−vis experiments in the absorption spectra of $H_2TPPS_4^{4-}$ at various surfactant/porphyrin ratios demonstrates the formation of different kinds of aggregates in solution, depending on the experimental conditions. Therefore, a detailed study on the porphyrin−surfactant interactions at surfactant concentrations below the cmc was performed.

At [surfactant]/[$H_2TPPS_4^{4-}$] = 4:1 and below the cmc (Figure 2) a strong decrease of the Soret band absorption together with a splitting with maxima at 408 and 418 nm is observed for both surfactants together with an ∼16 nm red shift of the two lowest energy Q-bands (absorbance values of Q-bands are given as Supporting Information). At [surfactant]/[$H_2TPPS_4^{4-}$] ≤ 3:1 for both the surfactants broadening and strong intensity decrease of the Soret band is observed (Supporting Information). Such spectral changes observed at surfactant concentration below cmc must be attributed to the formation of "premicellar" porphyrin−surfactant aggregates[8c,d] that we call here as porphyrin−surfactant heteroaggregates. The formation of a porphyrin−surfactant heteroaggregate was confirmed by fluorescence and resonance light scattering experiments (see below).

The fresh prepared diluted solutions of heteroaggregates show a symmetric splitting (±290 cm^{-1}) of the Soret band in two absorption bands of the same intensity. However, these equally intense bands evolve with time or with the increase of surfactant/porphyrin ratio to a higher intensity of the red-shifted band. This pattern of the Soret band arising from aggregation is significantly different from that observed in the typical π-stacking of the free base porphyrins (H-aggregation with a slightly hypsochromic shift) or in the side-to-side aggregation (J-aggregation with a bathochromic shift) characteristic of homoassociated diprotonated porphyrins. Therefore, the observed splitting indicates an uncommon geometrical arrangement of the porphyrins.

The porphyrin−surfactant heteroaggregate spectrum also was observed at higher porphyrin concentrations. For example, in the range of 0.1 μM ≤ [$H_2TPPS_4^{4-}$] ≤ 22.5 μM, at [**2**] = 1 mM (i.e., above the surfactant cmc), the absorption spectrum shows the split Soret band of the heteroaggregate (not shown). Moreover, the plot of the absorbance at the two Soret maxima as a function of porphyrin concentration is linear, thus indicating that the porphyrin−surfactant heteroaggregate is the only species in solution under these conditions. Note that the obtainment of heteroaggregates at concentration above the cmc implies that the formation of the heteroaggregate decreases the surfactant concentration below the cmc, thus suggesting either a higher stability of the heteroaggregates compared to that of the micelles or a kinetic barrier in the transformation of heteroaggregates into micelles. In contrast, previous results concerning analogous systems show that the premicellar aggregates disappear by increasing the surfactant concentration.[8c]

Fluorescence spectroscopy experiments confirm the presence of different species in solution depending on the [surfactant]/[$H_2TPPS_4^{4-}$] ratio. The emission spectra of the [$H_2TPPS_4^{4-}$] = 1 μM at some selected [surfactant]/[$H_2TPPS_4^{4-}$] ratios (for both the surfactants) are shown in Figure 3. The spectrum of $H_2TPPS_4^{4-}$ in water exhibits the characteristic two bands of the free base porphyrin at 644 and 704 nm (dashed line in Figure 3), but the presence of surfactant induces changes in the emission spectrum of the porphyrin showing the formation of new species. At [surfactant]/[$H_2TPPS_4^{4-}$] = 1:1 the emission spectrum (not shown) is very similar to that of porphyrin in water; however, at [surfactant]/[porphyrin] = 4:1, for both surfactants (**1** and **2**), the emission spectrum shows a strong decrease in quantum yield and a significant red shift of the emission maxima (657 and 721 nm) with respect to the spectrum of the porphyrin in

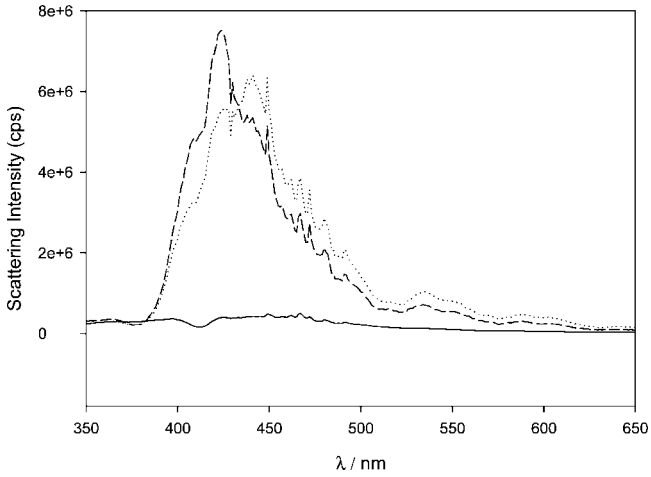

Figure 4. RLS profile of 1 μM $H_2TPPS_4^{4-}$, in the presence of surfactant **1a** (dotted line) and surfactant **2** (dashed line) at [surfactant]/[porphyrin] ratio of 4:1, compared with the RLS profile of porphyrin in water (solid line). Spectra are not corrected for photomultiplier response.

water. This, in agreement with the results obtained in the absorption experiments, demonstrates the formation of porphyrin−surfactant heteroaggregates at ∼4:1 [surfactant]/[porphyrin] ratio. Further, the lack of a dependence of the shape and the intensity of the emission spectra upon the excitation wavelength (and of the excitation spectra upon the selected emission wavelength) indicates the porphyrin−surfactant heteroaggregate as the highly predominant species in solution at this surfactant/porphyrin ratio.

At [surfactant]/[porphyrin] = 10 000:1 and surfactant concentration (10 mM), well above the cmc, a strong increase of the intensity of the emission spectrum was observed with the more intense maximum slightly blue-shifted with respect to the maximum of the emission spectrum of the sample 4:1 (650 and 717 nm, i.e., red-shifted with respect to the spectrum of free porphyrin in water). This result suggests the incorporation of monomeric porphyrin into the micelles. Note that, in the case of surfactant **2** (Figure 3b), the dependence of the intensity and of the wavelengths of the fluorescence maxima upon the selected excitation wavelength (at [surfactant]/[porphyrin] = 10 000:1) indicates the presence of both micellized porphyrin and porphyrin−surfactant heteroaggregate, in agreement with the results obtained in the UV−vis experiments. Actually, the simultaneous presence of heteroaggregate and micellized porphyrin in the solutions depends not only on the concentrations and their ratio but also on the hierarchical order of preparation of the two component solutions, which is discussed later.

Resonance light scattering (RLS)[5c,13] experiments gave further insight on the nature of the different species in solution. The evidence of the heteroaggregate in the RLS spectrum is the emergence of an intense scattering signal in the region of Soret absorption for both surfactants (Figure 4), thus indicating the presence of extended porphyrin arrays within the porphyrin−surfactant heteroaggregates, with long-range porphyrin interactions. On the other hand the monomeric micellized porphyrin (as well as the free monomeric porphyrin) shows no enhanced scattering in the Soret region; rather a minimum appears at the absorption maximum due to the self-absorption of the incident and scattered radiation.[13]

It is of note that the samples containing the porphyrin−surfactant heteroaggregate as main species at low $H_2TPPS_4^{4-}$ concentration (1 μM) show strong spectral changes as a function of time (decrease of the intensity and a broadening of the split Soret band) that suggest an organization of the porphyrin−surfactant heteroaggregates into larger aggregates (Figure 5, parts a and b). On the other hand, similar spectral changes are not observed when the porphyrin–surfactant heteroaggregates are formed at [$H_2TPPS_4^{4-}$] = 10 μM, at the same [surfactant]/[porphyrin] ratios (Figure 5, parts c and d).

However, porphyrin−surfactant large heteroaggregates (detected by the UV−vis) featuring the characteristic broad spectrum shown in Figure 5, parts a and b, were also obtained at [$H_2TPPS_4^{4-}$] = 10 μM (at [**2**]/[$H_2TPPS_4^{4-}$] = 6:1 by adding successive proper amounts of concentrated surfactant and porphyrin solutions to a previously equilibrated solution of 1 μM $H_2TPPS_4^{4-}$ and 6 μM **2**, i.e., containing large heteroaggregates. The experiment was carried out by adding to the preformed heteroaggregate, first the surfactant and then the porphyrin concentrated solution. After each addition the sample was allowed to equilibrate for 1−2 h following the evolution into larger aggregates by the decrease of intensity in the absorption spectra. The UV spectra, performed at different times after each addition, are reported as Supporting Information. Noteworthy, the addition of the surfactant to a solution containing porphyrin−surfactant heteroaggregates does not induce any spectral change, i.e., it does not perturb the heteroaggregate structure, whereas the addition of the concentrated porphyrin solution induces the formation of new small heteroaggregates (featuring a more intense absorption) that slowly organize into larger aggregates. Finally, we observed that the growth to larger heteroaggregates is faster in the presence of preformed large heteroaggregates. The hydrophobic effect plays an important role in the formation of the heteroaggregates and in the kinetics of the aggregation, as shown in the following experiment. In a fresh prepared solution at [$H_2TPPS_4^{4-}$] = 2.5 μM and [**2**]/[porphyrin] = 4:1 the increase of temperature irreversibly promotes aggregation (Figure 6), thus demonstrating that the driving force of the heteroaggregation process is the hydrophobic effect (direct relationship with temperature) and that the formation of the heteroaggregates is irreversible.

A Job's plot analysis allowed us to determinate the stoichiometry of the porphyrin−surfactant heteroaggregates. Figure 7 shows the plot obtained for **1a** by plotting absorbance at 416 nm versus the porphyrin molar fraction (10 μM, total concentration). The minimum was obtained at porphyrin molar fraction 0.25 corresponding to an unexpected surfactant/porphyrin 3:1 stoichiometry. An analogous result was obtained for surfactant **2**.

This stoichiometry implies that the porphyrin building block in the aggregate features a free sulfonato group able to interact with water and that hydrophobic interactions between the hexadecyl tails of neighboring surfactant molecules can construct an organized hydrophobic network (Scheme 1). A parallel array of two one-dimensional (1D) chains (Scheme 1) explains the 3:1 stoichiometry as the consequence of the stabilization exerted by the formation of polar surfaces that interact with water, and that would not occur at a 4:1 stoichiometry. However, the asymmetric shape of the Job's plot suggests the formation of aggregates with stoichiometry between 3:1 and 4:1. On the basis of the changes observed, as a function of time and/or temperature, in the UV−vis spectra of porphyrin−surfactant heteroaggregates at surfactant/porphyrin ratios >3:1, the hypothesis is that the heteroaggregate would grow once formed the 3:1 bilayer by incorporating 4:1 layers between the external layers

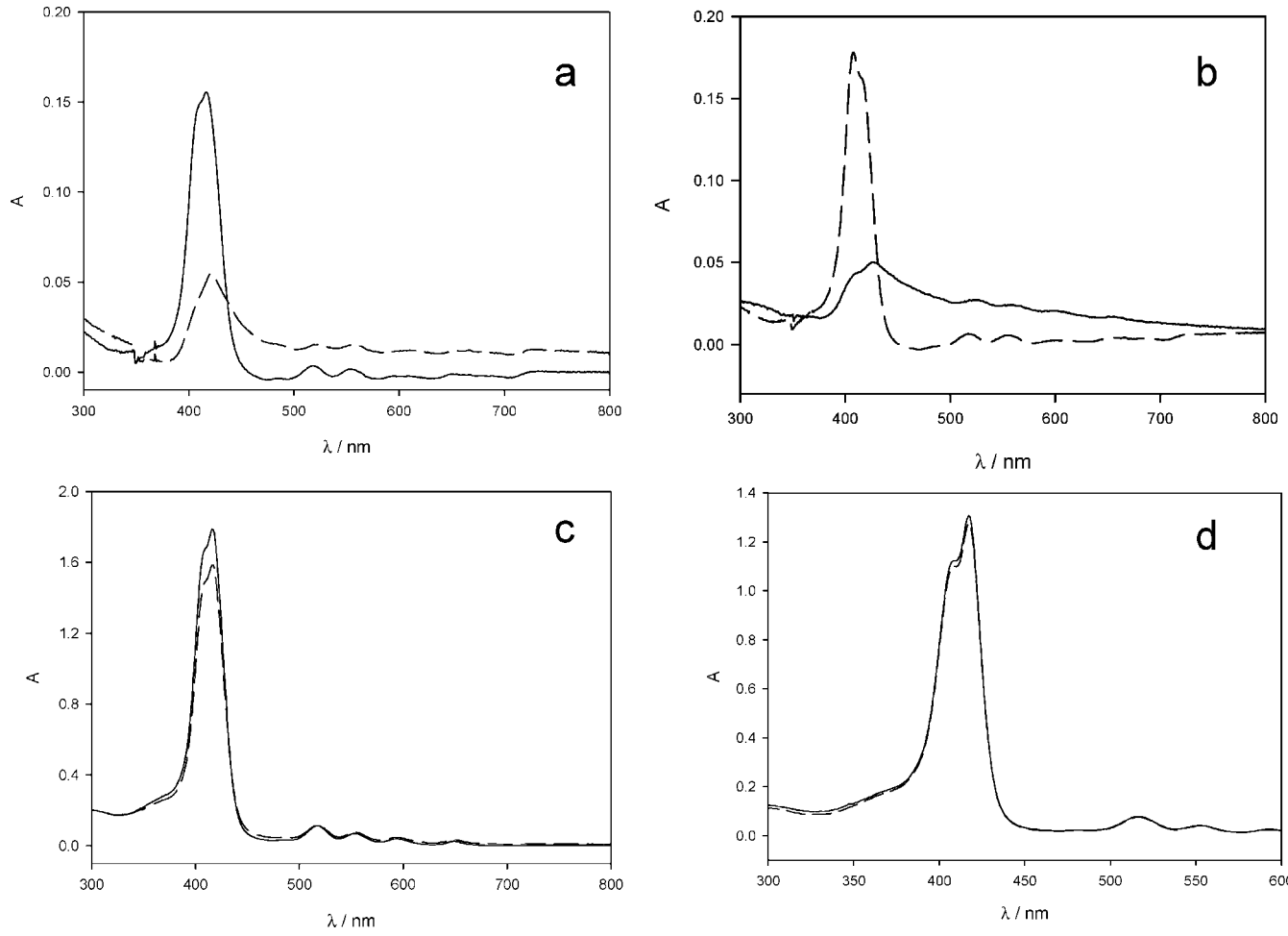

Figure 5. UV−vis spectrum of the surfactant−porphyrin heteroaggregates at [surfactant]/[porphyrin] ratio of 6:1, at $t = 0$ (solid line) and $t = 24$ h (dashed line), (a) at $[H_2TPPS_4^{4-}] = 1$ μM in the presence of surfactant **1a**; (b) at $[H_2TPPS_4^{4-}] = 1$ μM in the presence of surfactant **2**; (c) at $[H_2TPPS_4^{4-}] = 10$ μM in the presence of surfactant **1a**; (d) at $[H_2TPPS_4^{4-}] = 10$ μM in the presence of surfactant **2**.

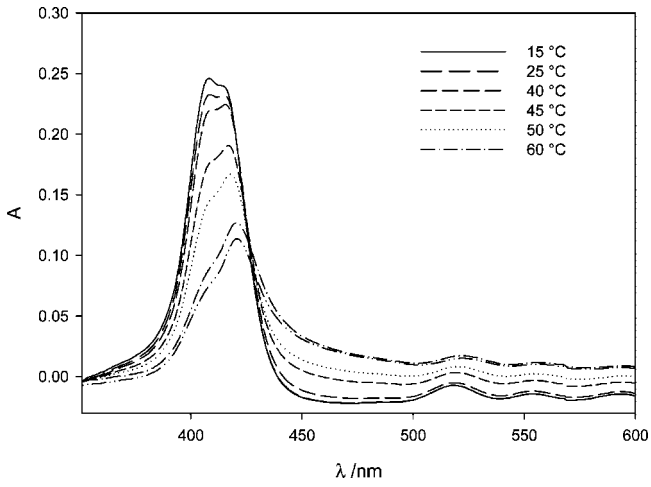

Figure 6. UV−vis spectrum of 2.5 μM $H_2TPPS_4^{4-}$ in the presence of surfactant **2** at [surfactant]/[porphyrin] ratio of 4:1 taken at different temperatures, starting from 15 °C and increasing up to 60 °C.

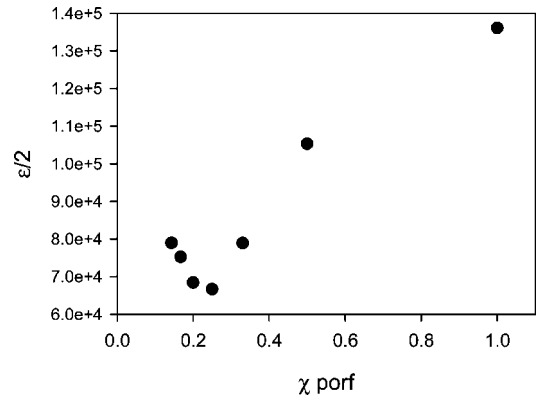

Figure 7. Job plot relative to the porphyrin−surfactant **1a** heteroaggregate, obtained by plotting absorbance at 416 nm vs porphyrin molar fraction.

of 3:1 stoichiometry. This would lead to an overall stoichiometry between 3:1 and 4:1.

Notice that an orthogonal arrangement of the 2D networks reported in Scheme 1, with the hexadecyl chains crossing the cavities occurring in the 2D network between four porphyrin sites, would give a 3D structure. Such a structure would explain the kinetic reluctance of the heteroaggregates to transform into micelles incorporating the porphyrin as put in evidence by the experiments discussed below. This irreversibility suggests a hierarchical aggregation process which is confirmed by the dependence of the aggregation on the order of mixing. In fact, we could observe that in the case of surfactant **1a** at surfactant concentration above the cmc the type of the obtained aggregates also depends on the protocol of the sample preparation (Figure 8a). Actually, the dissolution of the surfactant powder in a dilute porphyrin solution yields micellized monomeric porphyrin,

Scheme 1

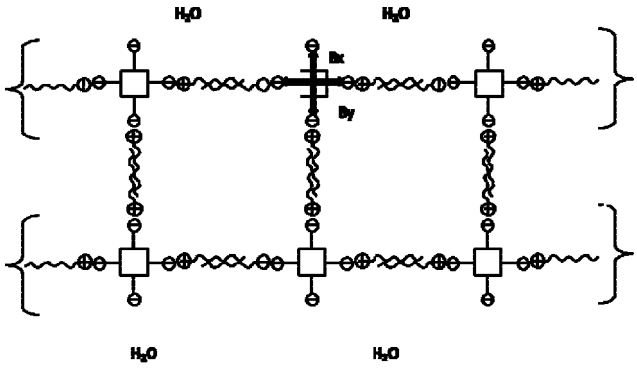

whereas the addition of a concentrated porphyrin solution to a micellar solution gives the formation of the heteroaggregate. Sonication of both samples does not produce any spectral change, and samples remain unchanged for days, thus showing that there is no interconversion between the two kinds of aggregates. However the interconversion of heteroaggregates into porphyrin including micelles was obtained by precipitation at low temperature of the surfactant from heteroaggregate followed by redissolution. In the case of surfactant **2** both protocols of sample preparation yield the formation of the porphyrin−surfactant heteroaggregate as the most abundant species (Figure 8b).

Transfer of Chirality. Our principal objective being to detect the transfer of chirality from the chiral surfactant to the achiral porphyrin, the investigation described previously was necessary in order to detect unambiguously the species occurring in solution.

$H_2TPPS_4^{4-}$ solutions in the presence of the chiral ammonium salt **3** (at [**3**]/[$H_2TPPS_4^{4-}$] ratio ranging between 1 and 22) are CD silent in the region of the porphyrin absorption bands. This was an expected result as consequence of the absence of electronic perturbations between surfactant and porphyrin.

The CD experiments on the porphyrin/surfactant samples were carried out at [$H_2TPPS_4^{4-}$] = 10 μM (i.e., a concentration that ensures proper absorbance values) on two type of samples: monomeric micellized porphyrin at [surfactant]/[porphyrin] = 250:1 prepared in conditions were the heteroaggregate is absent; samples of surfactant−porphyrin heteroaggregate ([surfactant]/[porphyrin] at 4.1 and 6:1 ratios).

Unexpectedly, the micellized porphyrin is CD silent for both surfactants. This result excludes porphyrin as a probe of chirality of these chiral micellar aggregates. Actually, the porphyrin in the chiral micelle features an electronic perturbation (as seen in the UV−vis spectrum), but the structural arrangement of the porphyrin in the micelle is probably a racemic mixture of conformational chiral porphyrin structures, because a loose interaction with the chiral aggregate does not allow a diastereoselection. In contrast, the heteroaggregate shows intense bisignate bands at the absorption wavelengths of the porphyrin (Figure 9). As expected the sign of the CD bands is opposite in the CD spectra of the heteroaggregates formed by the surfactant enantiomers (Figure 10).

The CD spectra of the large porphyrin−surfactant heteroaggregates obtained at [$H_2TPPS_4^{4-}$] = 10 μM by the protocol described above also show a bisignate band, similar to the band obtained for the smaller heteroaggregates. The intensity of CD spectrum of the solution obtained immediately after the last addition of the concentrated surfactant and porphyrin solutions decreases as a function of time, analogously to what is observed in the absorption spectra (decrease and broadening of the band). This change must be attributed to the increase of the size of the aggregate leading to an apparently lower extinction coefficient. Interestingly a clear isodichroic point is observed for the CD spectra registered at different times (Supporting Information), thus suggesting that the structural motif responsible for the CD band is the same in the small and in the large heteroaggregates.

With respect to the structure of the porphyrin chromophore leading to the CD response, note that the 3:1 stoichiometry must lead to the breaking of the degeneracy of the *x* and *y* electronic transitions (Scheme 1). Actually, in the porphyrin−surfactant heteroaggregate the anisotropic interactions on the macrocycle periphery (Coulombic interactions in one directions and water/Coulombic on the other) would differentiate the two degenerate Soret B_x and B_y transitions of the symmetric porphyrin, as seen in the UV−vis spectrum.[6,7] The presence of chiral surfactants on the periphery of the achiral porphyrin simply transforms it in a chiral, optically active, chromophore by stabilizing the phenyl group conformational angles in one of the two enantiomorphous forms. As a consequence, the B_x and B_y transitions are CD active. The rigidity of the heteroaggregate structure surely plays a decisive role in the transfer of chirality (diastereoselection). Note that the chiral transfer is not due the chiral induction exerted in homoassociates, as is the case of the well-known J-aggregates of this type of porphyrin, but rather to the formation of heteroassociates with defined structural trends.

Concluding Remarks

We have investigated the interaction of two chiral cationic surfactants with an achiral anionic porphyrin. Depending on the experimental conditions these may result either in the inclusion of the monomeric porphyrin in the micellar aggregates of the surfactant or in the formation of porphyrin−surfactant heteroaggregates whose absorption spectrum is characterized by a split of the Soret band centered at 413 nm. The fact that above the cmc different protocols of mixing the porphyrin and surfactant **1** yield either micelles including monomeric porphyrin or porphyrin−surfactant heteroaggregates which do not interconvert indicates the complexity of the dynamics of the overall system. In fact, though micelles are equilibrium systems in fast exchange with the monomeric surfactant, the inclusion of $H_2TPPS_4^{4-}$ in the micelles is almost irreversible, due to the high association constant of the porphyrin with the micellar aggregates. Further, though the formation of the 1:3 porphyrin−surfactant structural motif is probably reversible, its hierarchical aggregation into more complex and organized heteroaggregates driven by hydrophobic interactions is also irreversible. Similar effects, only understandable assuming a hierarchical association, have been described for the homoassociation of $H_2TPPS_4^{4-}$ and similar water-soluble porphyrins.[3d,h,i] This is in contrast with the multiple equilibrium picture invoked previously in the interaction of $H_2TPPS_4^{4-}$ other cationic surfactants (e.g., CTAB).[8c,d] However, in the case of surfactant **2**, the formation of the porphyrin−surfactant heteroaggregates occurs more easily also in the conditions in which **1** yields micellar aggregates including monomeric porphyrin, thus demonstrating a fundamental role of the molecular structure of the surfactant in the building and in the organization of the heteroaggregates, as demonstrated also by the pattern of CD spectra.

We found that hydrophobic interactions have a fundamental role in the formation of the heteroaggregates; further, for both

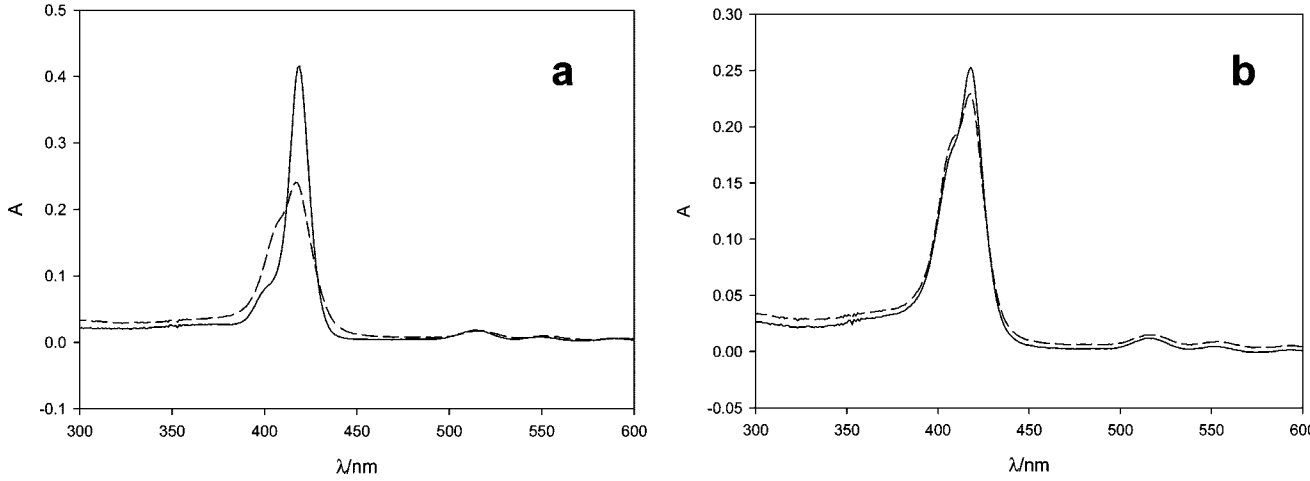

Figure 8. UV−vis spectrum of 1 μM $H_2TPPS_4^{4-}$ in the presence of surfactant **1a** (a) and **2** (b) at [surfactant]/[porphyrin] ratio of 2500:1 prepared (i) by dissolving the surfactant powder in a dilute porphyrin solution (solid line) and (ii) by adding a concentrated porphyrin solution to a micellar solution (dashed line).

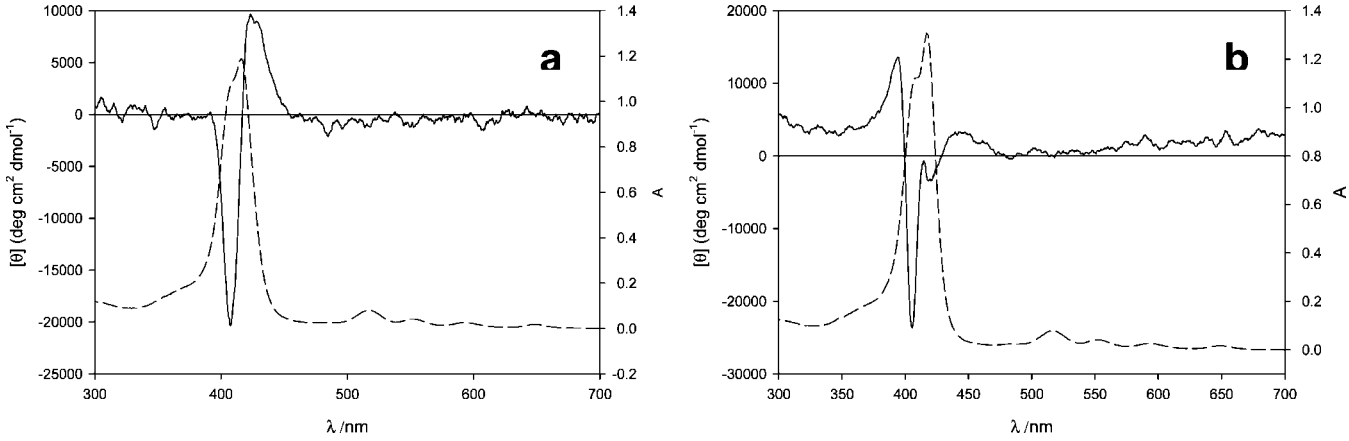

Figure 9. CD spectrum (solid line) and UV−vis spectrum (dashed line) of 10 μM $H_2TPPS_4^{4-}$ at [surfactant]/[porphyrin] ratio of 6:1 in the presence of surfactants **1a** (a) and **2** (b).

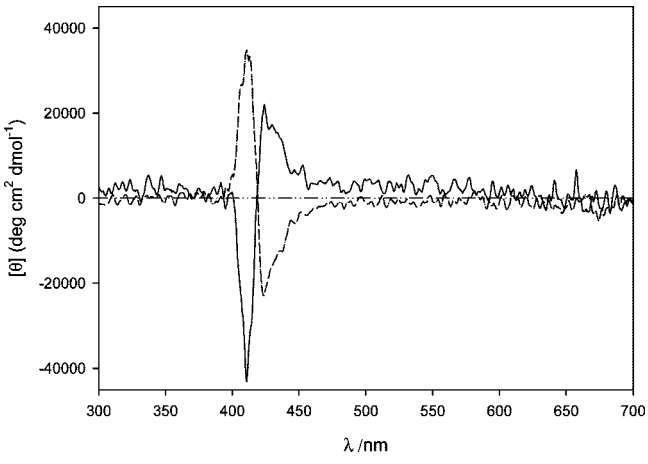

Figure 10. CD spectrum of 12.5 μM $H_2TPPS_4^{4-}$ at [surfactant]/[porphyrin] ratio of 4:1 in the presence of surfactants **1a** (solid line) and **1b** (dashed line).

surfactants the (surfactant/porphyrin) stoichiometry in the heteroaggregates is 3:1, thus leaving a sulfonate group free to interact with water and confirming the lyotropic-like liquid crystal behavior of ionic amphiphilic porphyrins.[9] We also observed a progressive hierarchical association of the heteroaggregates (formed at [porphyrin] = 1 μM) into larger aggregates characterized by a decrease of intensity, by a broadening of the split Soret band as a function of time, and finally, by an increase of the stoichiometry from 3:1 toward 4:1. Because of its organization, the heteroaggregate is therefore an excellent model for investigating the transfer of chirality from molecules to complex systems. Actually, the porphyrin embedded in the heteroaggregate, differently from the porphyrin included in micellar aggregates, features a bisignate CD band, thus demonstrating that due to tight interactions in the highly organized system governed by Coulombic and hydrophobic interactions, both chiral surfactants are able to transfer their stereochemical information to the whole aggregate by selecting one of the enantiomeric forms of the porphyrin where phenyl groups are tilted with respect to orthogonality. We do not know the extent of enantioselection (i.e., the extent of enantiomeric excess); however, the important point is the finding of transfer of chirality in systems controlled by a combination of Coulombic and hydrophobic interactions; in fact, neither Coulombic or hydrophobic interactions per se were shown to be sufficient to observe it.

A further point of interest is given by the fact that the formation of the highly organized porphyrin−surfactant heteroaggregates occurs at very low concentration of components. This highlights the possibility that very low concentrations of amphiphiles in the primordial soup might have been sufficient

to settle the conditions of organization and recognition necessary for the development of life and might have had a role on the history of chiral homogeneity of biomolecules.

Acknowledgment. We express thanks for the financial support from Dipartimeto di Progettazione Molecolare and from the Spanish Government project AYA2006-1648-C02-01. A.S. thanks COST Action D27 for an STMS travel bourse. We thank Professor Roberto Purrello for the communication of unpublished results on the hierarchical dependence on the mixing of the components in noncovalent synthesis of aggregates of amphiphilic porphyrins.

Supporting Information Available: Absorption spectra (Soret region) of 1 μM $H_2TPPS_4^{4-}$ at various [surfactant]/[porphyrin] ratios for both the surfactants, wavelengths of the Q-bands for the same absorption spectra, and UV−vis and CD spectra of the large porphyrin−surfactant heteroaggregates (at $[H_2TPPS_4^{4-}] = 10\ \mu$M) performed at different times. This material is available free of charge via the Internet at http://pubs.acs.org.

JA805669V